Mössbauer study of the kinetics of the amorphous-to-crystalline transformation in amorphous $Fe_{81}B_{13.5}Si_{3.5}C_2$

N. Saegusa* and A. H. Morrish
Department of Physics, University of Manitoba, Winnipeg, Manitoba R3T 2N2, Canada
(Received 1 November 1982)

Transmission Mössbauer spectra were recorded during isothermal annealing in order to study kinetic aspects of the amorphous-to-crystalline transformation in amorphous $Fe_{81}B_{13.5}Si_{3.5}C_2$ (Metglas® 2605SC). The crystalline products are Fe-Si alloy, Fe_2B, and Fe_3C after annealing at 706 K for 6.72×10^5 s. Crystallization proceeds in at least two steps. In the first step an Fe-Si alloy precipitates at a rate that becomes slower with time. Simultaneously, paramagnetic and magnetically ordered amorphous phases coexist; the ordered phase then increases with time at the expense of the paramagnetic phase. It is concluded that after crystallization starts, the amorphous phase first becomes nonuniform in atomic composition, and then later, but before the second crystallization step, develops into a quasistable homogeneous state.

I. INTRODUCTION

The amorphous-to-crystalline transformation of metallic glasses is a subject of current interest. Recently, this transformation in isochronally annealed $Fe_{81}B_{13.5}Si_{3.5}C_2$ ribbons (Metglas® 2605SC) was reported to be a multistep process.[1] However, since the transformation to a crystalline material depends on time as well as temperature, a determination of the changes during isothermal annealing is desirable. Such results should provide information on the dynamics of the processes involved. Consequently, a series of Mössbauer spectra have been obtained during the isothermal annealing of $Fe_{81}B_{13.5}Si_{3.5}C_2$ at several temperatures ranging between 640 and 706 K. The hyperfine parameters and absorption areas have been deduced and utilized in the analyses of the amorphous-to-crystalline transformation.

II. EXPERIMENTAL

Amorphous $Fe_{81}B_{13.5}Si_{3.5}C_2$ (Metglas® 2605SC) in a continuous ribbon form of 25.4-mm width and 30-μm nominal thickness was obtained from the Allied Corporation (U.S.A). Samples approximately 18×18 mm^2 were cut from the ribbon. Mössbauer spectra were recorded with a conventional constant-acceleration spectrometer. Calibration was made with a natural α-Fe foil. A conventional vacuum furnace was used for annealing and *in situ* Mössbauer spectra were obtained. The vacuum was always maintained to better than 10^{-5} Torr during the heating period. The furnace was heated from room temperature to the annealing temperature in approximately 50 min (3.00×10^3 s). Special care was taken to minimize the overshooting of the temperature upon attaining the annealing temperature. The maximum overshooting was about 5 °C for less than 3 min. The temperature of the furnace was kept within ±2 °C for the remainder of the annealing time.

The absorption lines of the amorphous and crystalline phases were fitted with quasi-Lorentzian[2] and Lorentzian line shapes, respectively. For six-line magnetic spectra, the areas were constrained with $A_i=A_{7-i}$ ($i=1,2,3$), where A_i is the absorption area of the ith line. For paramagnetic doublets, the areas of the two lines were constrained to be equal. In order to aid in the fitting, the patterns for the crystalline components were constrained to be in the ratio $A_1:A_2:A_3=3:2:1$, which corresponds to random orientation of the magnetic moments. This assumption was found to be valid for the phases with well-resolved first, second, fifth, and sixth lines. The linewidths Γ_i ($i=1,2,3,\ldots,6$) were constrained to be $\Gamma_1:\Gamma_2:\Gamma_3:\Gamma_4:\Gamma_5:\Gamma_6=1:0.92:0.89:0.89:0.92:1$, which corresponds to the ratios observed for a 6.4-μm-thick α-Fe foil. More specific fitting procedures employed are discussed in the relevant section.

III. RESULTS AND DISCUSSION

Five different isothermal annealing temperatures T_A were used, namely, 640, 670, 684, 696, and 706 K. The annealing time t_A is defined as the time elapsed after reaching the chosen annealing tempera-

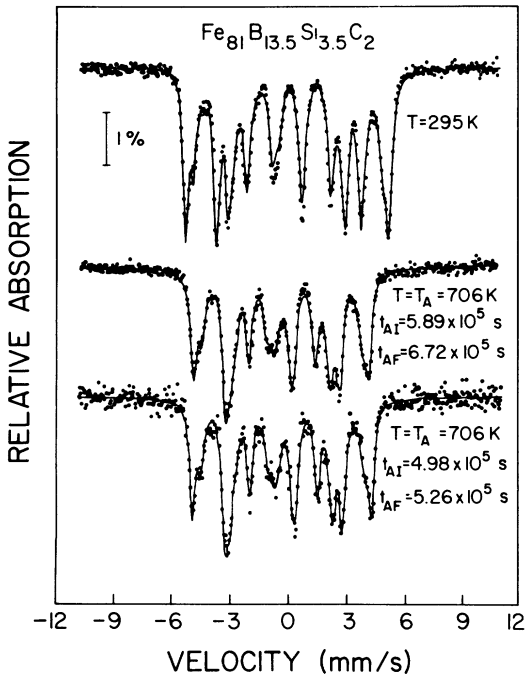

FIG. 1. Mössbauer spectra of completely crystallized $Fe_{81}B_{13.5}Si_{3.5}C_2$ ribbon. The spectrum at the top was recorded at 295 K after annealing at 706 K for 6.72×10^5 s. The two spectra at the bottom were recorded during isothermal annealing at 706 K between the initial and final times t_{AI} and t_{AF}, respectively, as indicated.

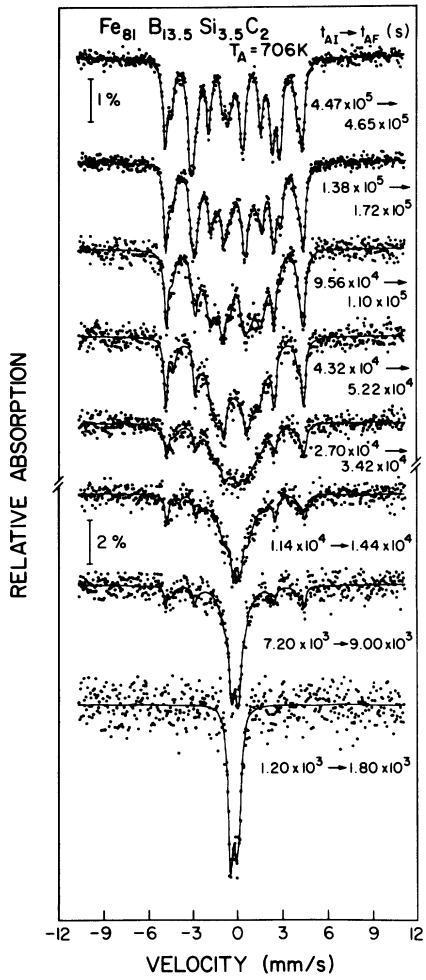

FIG. 2. Mössbauer spectra of amorphous $Fe_{81}B_{13.5}Si_{3.5}C_2$ ribbon during isothermal annealing at 706 K. The indicated initial and final annealing times t_{AI} and t_{AF}, respectively, are measured upon reaching $T_A=706$ K after heating from 295 K.

ture. It should be noted that atomic rearrangements take place during the heating-up period. Thus the amorphous state at $t_A=0$ in the present measurements will have already changed from the as-quenched state. Therefore, the actual annealing time is longer than the t_A values quoted in this present study. The error from this source will become smaller as t_A becomes larger.

Another source of error is the finite time required to obtain a spectrum with reasonable counting statistics. Since the amorphous-to-crystalline transformation is an irreversible process, the crystalline fraction will never decrease with an increase in t_A. Hence the crystalline fractions for a certain t_A tend to be underestimates because the data are a time average between the initial time t_{AI} and the final time t_{AF} (equal to t_A, as used in the data analyses), where $t_{AI}=t_{AF}-t_{acc}$, and t_{acc} is the accumulation time for one spectrum. A correction for this error could be made if the time dependence of the crystalline fraction, which is to be determined with the data, is known. A correction could possibly be made by reducing the quoted value of t_A using the appropriate crystallization rate. This correction would be in the opposite direction to the error that has its origin in the finite heating-up time. However, in view of the complexity of these errors, no corrections have been made to t_A in the present study.

A. Crystalline products

A sample was completely crystallized after annealing at $T_A=706$ K for $t_A\geq2.84\times10^5$ s. A Mössbauer spectrum was recorded at 295 K after annealing for $t_A=6.72\times10^5$ s at 706 K and is shown in Fig. 1. Also shown are spectra collected at 706 K *in situ* between the times t_{AI} and t_{AF}, as stated in the figure; they confirm that the crystallization

TABLE I. Magnetic hyperfine fields H_{hf}, isomer shifts δ, quadrupole shift ϵ, relative areas, and assignments of patterns of crystalline phases (1–5) after complete crystallization of amorphous $Fe_{81}B_{13.5}Si_{3.5}C_2$. The parameters at 295 K were obtained after the sample had been annealed at $T_A = 706$ K for 6.72×10^5 s; those at 706 K were recorded during annealing starting at the initial time of $t_{AI} = 5.89 \times 10^5$ s and ending at the final time of $t_{AF} = 6.72 \times 10^5$ s, both measured from the time the annealing temperature was reached.

T(K)		1	2	3	4	5
295	H_{hf} (T)	33.07	30.76	27.87	23.50	
	δ (mm/s)	0.055	0.097	0.12	0.16	
	Relative area (%)	34.0	19.7	3.6	42.7	
	assignment	Fe-Si (8NN)	Fe-Si (7NN)	Fe-Si (6NN)	Fe_2B	
706	H_{hf} (T)	28.49	26.13		18.64	
	δ (mm/s)	−0.25	−0.20		−0.15	−0.06
	ϵ (mm/s)					0.67
	Relative area (%)	31.1	21.5		40.3	7.0
	assignment	Fe-Si (8NN)	Fe-Si (7NN)		Fe_2B	Fe_3C

was complete for $t_A \geq 2.84 \times 10^5$ s. The hyperfine parameters and relative areas deduced for each pattern are tabulated in Table I. The hyperfine fields and isomer shifts at 295 K after the 706-K anneal are very similar to those obtained in the isochronal annealing study[1]; the same two crystalline products are identified, namely the alloy Fe-Si and the compound Fe_2B.

In Table I it may be noted that for the Fe-Si alloy, a pattern for Fe with six Fe nearest neighbors (6NN) was not fitted at 706 K. Apparently, either the Fe-Si alloy has fewer 6NN sites at 706 K or the relative area of the 6NN Fe pattern is not large enough to be successfully fitted, given the statistics of the data. In view of the relatively small area associated with the 6NN sites at 295 K, the small number of counts collected at 706 K is probably the reason. Pattern 5, which is a paramagnetic doublet at 706 K, is assigned to crystalline Fe_3C. The quadrupole splitting of pattern 5 is consistent with the weighted average of the values reported in the literature.[3] The magnetic ordering temperature of crystalline Fe_3C is 483 K.[4] However, a pattern for Fe_3C was not identified at 295 K, partly because the resolution was inadequate, and partly because the area was relatively small. In summary, the crystalline products of $Fe_{81}B_{13.5}Si_{3.5}C_2$ are an Fe-Si alloy, Fe_2B and Fe_3C.

B. Amorphous-to-crystalline transformation

In the time scale of the present isothermal annealing experiments, the onset of bulk crystallization was observed for $T_A \geq 640$ K and complete crystallization was only attained for $T_A = 706$ K. Mössbauer spectra at 706 K, successively recorded between the times t_{AI} and t_{AF} indicated, are shown in Fig. 2. The spectra are very complex because the amorphous and crystalline patterns overlap. In order to get convergence in the fitting procedure, the quasi-Lorentzian line shapes of the magnetically ordered amorphous pattern were constrained to be the same for all six lines. The absorption areas ($\sum_{i=1}^{6} A_i$) of the amorphous and crystalline patterns

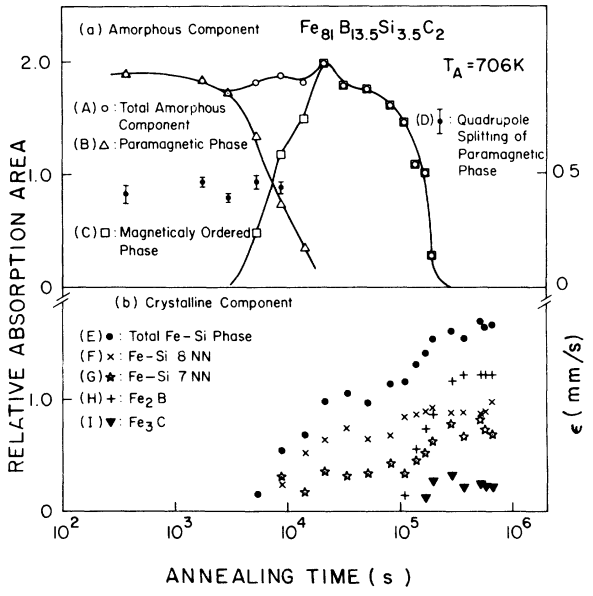

FIG. 3. Absorption areas of the patterns for the (a) amorphous and (b) crystalline phases during the isothermal annealing of amorphous $Fe_{81}B_{13.5}Si_{3.5}C_2$ at $T_A = 706$ K. The quadrupole splittings ϵ together with error bars of the paramagnetic amorphous phase are also shown.

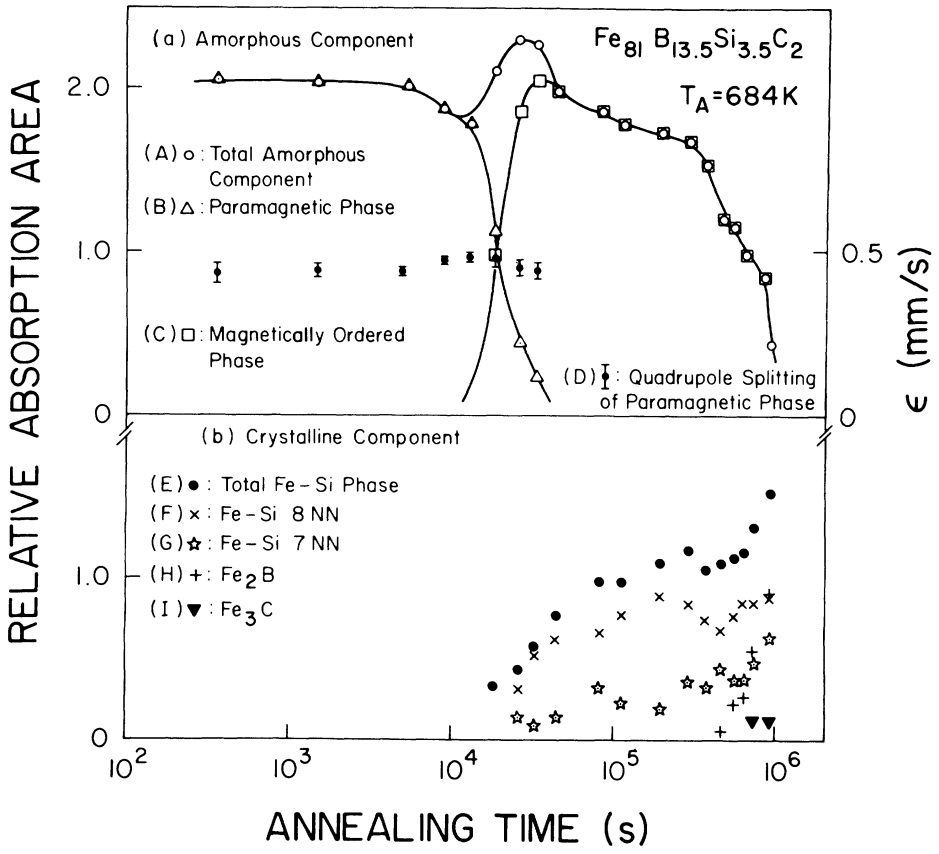

FIG. 4. Absorption areas of the patterns for the (a) amorphous and (b) crystalline phases during isothermal annealing of amorphous $Fe_{81}B_{13.5}Si_{3.5}C_2$ ribbon at $T_A=684$ K. In addition, ϵ for the paramagnetic amorphous phase is plotted.

are plotted as a function of the annealing time t_A (equal to t_{AF}) for $T_A=706$ and 684 K in Figs. 3 and 4, respectively. The plots for the other annealing temperatures are similar. The lower the annealing temperature is below 706 K, the longer the time required for the start of crystallization becomes.

It should be noted that the recoilless fraction f_R of a pattern may not remain the same during the isothermal annealing. In particular, f_R of the amorphous component might change during the amorphous-to-crystalline transformation inasmuch as an increase of $\sim 8\%$ was observed at 295 K after isochronal annealing.[1] Indeed, the variation of the total amorphous area with t_A (Figs. 3 and 4) does indicate that f_R increases at the early stages of crystallization. Any change of f_R for the crystalline components is expected to be smaller since the crystalline structure is well defined after the transformation; however, no experimental data are available to support this assumption.

The onset of crystallization is heralded by the precipitation of an Fe-Si alloy. Thereafter, the crystallization of Fe_2B occurs, and then finally Fe_3C becomes detectable. Because the area of the Fe_3C component is relatively small, resolution of this pattern is difficult, especially in the early stages.

In order to study the kinetics of the amorphous-to-crystalline transformation, the dependence of the crystalline fractions on annealing time have been analyzed employing the Johnson-Mehr-Avrami equation,[5]

$$x(t_A)=1-\exp(-k_n t_A^n)\,, \tag{1}$$

where k_n is a temperature-dependent constant and n characterizes the crystallization process. A log-log plot of $\ln 1/(1-x)$, where x is $x(t_A)$ in Eq. (1) versus the annealing time t_A gives a straight line with slope n.

The crystalline fractions $x(t_A)$ are given by the absorption areas,[6] providing that the crystalline recoilless fractions do not change during the isothermal annealing. Johnson-Mehr-Avrami plots for

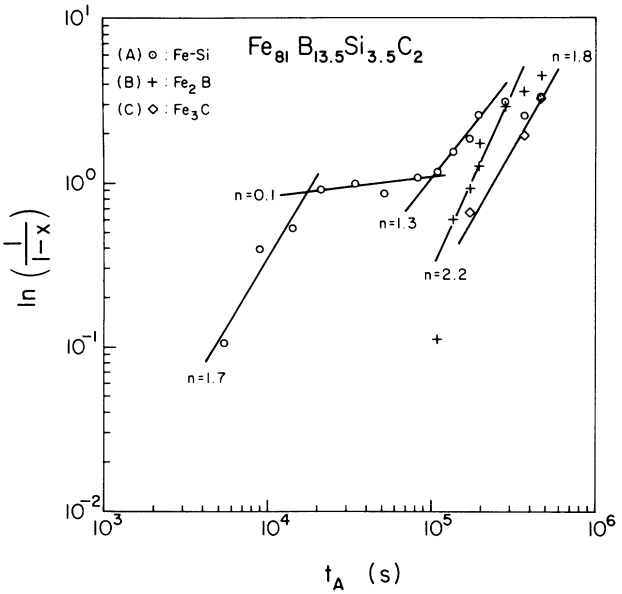

FIG. 5. Johnson-Mehr-Avrami plot for Fe-Si, Fe_2B, and Fe_3C.

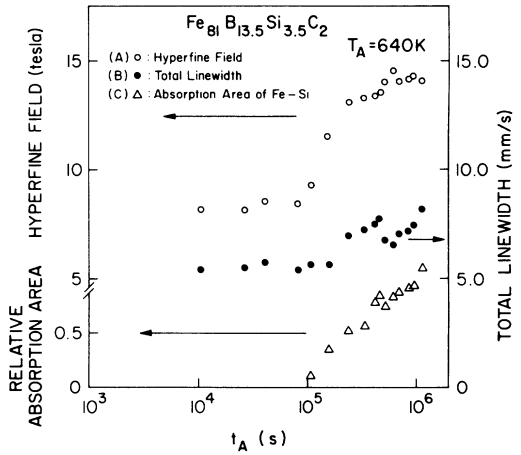

FIG. 6. Hyperfine fields and total linewidths of the amorphous component together with the total absorption area of the crystalline Fe-Si phase as a function of t_A during isothermal annealing at $T_A = 640$ K.

Fe-Si, Fe_2B, and Fe_3C at $T_A = 706$ K are shown in Fig. 5. For the Fe-Si alloy, $n = 1.7$ during the early stages of crystallization, and then decreases to $n = 0.1$, indicating that the crystallization is slowing down. Then, beginning with the start of crystallization of Fe_2B, n for Fe-Si increases and becomes 1.3. For Fe_2B, n is determined to be equal to 2.2. For Fe_3C, n is found to be 1.8, although now the error is much larger because the area of this pattern is rather small.

The amorphous-to-crystalline transformation mechanism depends on the value of n.[7] However, n itself is a sum of more than one term, so that for any given value of n several different models are possible. Although the values of n for Fe-Si, Fe_2B, and Fe_3C during the second stage of crystallization ($t_A > 10^5$ s in Fig. 5) could be used to indicate the amounts of the these three crystalline components, the lack of accuracy in n requires that caution be exercised.

Additional information during the amorphous-to-crystalline transformation can be obtained by considering Mössbauer parameters of the amorphous phase. The hyperfine field and the total linewidths ($\sum_{i=1}^{6} \Gamma_i$) of the amorphous component together with the total absorption area of crystalline Fe-Si component are shown as a function of t_A for $T_A = 640$ K in Fig. 6. The rapid increase in H_{hf} correlates with the growth of the crystalline phase. Now, after precipitation of the iron-rich crystalline Fe-Si alloy begins, the atomic composition of the amorphous component will become metalloid rich in comparison to the as-quenched amorphous ribbon. Hence, in the amorphous component, the magnetic moment of the iron atoms will decrease and the magnetic ordering temperature T_F will increase.[8] Since the hyperfine field is generally proportional to the magnetic moment,[9] the increase of H_{hf} in Fig. 6 establishes that T_F of the amorphous phase increases after the onset of crystallization.

In addition, the total linewidth of the pattern for the amorphous component increases after crystallization begins; this observation indicates that the distribution in H_{hf} becomes larger, at least during the early stages of the amorphous-to-crystallization process. However, at about $t_A = 5 \times 10^5$ s, the slight decrease in the total linewidth may indicate that the H_{hf} distribution then becomes smaller.

In a thermal scan using a heating rate of 5 K/min, the Curie temperature of as-quenched amorphous $Fe_{81}B_{13.5}Si_{3.5}C_2$ was determined to be $T_F = 668 \pm 2$ K.[10] In the present isothermal annealing experiment, a paramagnetic doublet for the still totally amorphous ribbon was observed initially when the annealing temperature T_A was equal to or higher than 670 K. After crystallization begins, an extra pattern with broad quasi-Lorentzian line shapes, and hence corresponding to another amorphous component, is required to fit the data. This extra pattern is first a singlet, but changes to a doublet and finally to a sextet with an increase in the annealing time t_A. Then as t_A increases further, the area of this extra pattern grows, whereas the area of

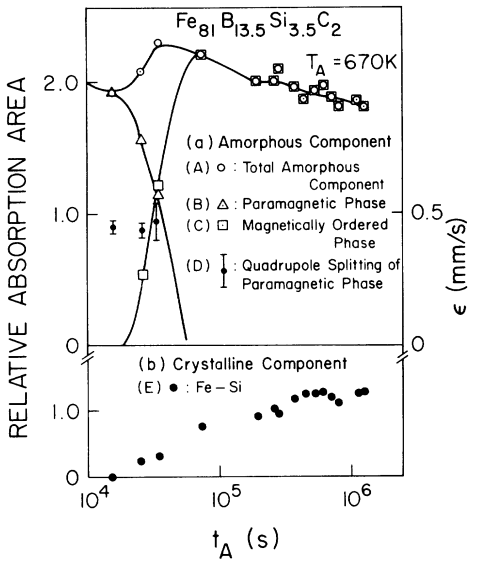

FIG. 7. Relative absorption areas of the patterns for the (a) amorphous and (b) crystalline components during isothermal annealing at $T_A = 670$ K. Also shown is ϵ vs t_A for the paramagnetic amorphous phase.

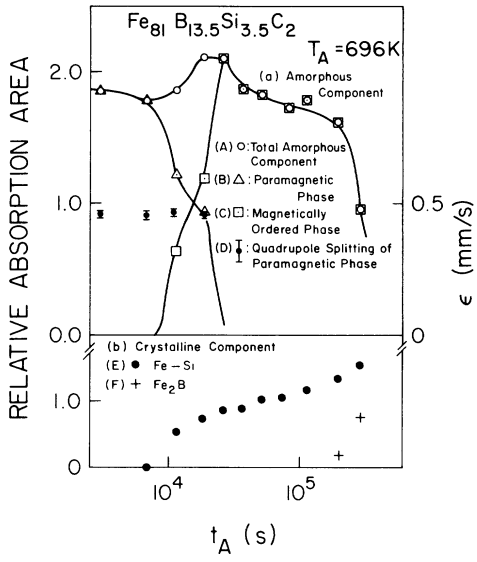

FIG. 8. Similar to Fig. 7 except that the isothermal annealing temperature now is 696 K.

the initial paramagnetic doublet decreases. The spectral areas of the paramagnetic and the magnetically split phases of the amorphous component, together with the various crystalline phases, are plotted as a function of the annealing time t_A for $T_A = 670$, 684, 696, and 706 K in Figs. 7, 4, 8, and 3, respectively.

The following model is proposed. The initial paramagnetic doublet for $T_A = 670$ K, which is very close to $T_F = 668 \pm 2$ K, persists for a lengthy time (until $t_A \approx 2 \times 10^4$ s). Further, the doublet's hyperfine parameters change but little with annealing time for any of the annealing temperatures used. Therefore, it seems probable that the atomic composition of this amorphous component remains the same, or almost the same, as that of the as-quenched ribbon.

Just after crystallization commences, localized crystalline nuclei form that have been identified by electron microscopy.[11] The growth of the Fe-Si crystallites is suggested to continue by the consumption of nearby iron atoms. As a consequence, the atomic composition of the surrounding amorphous phase becomes metalloid rich. The result is that an additional amorphous pattern is observed. It becomes magnetically split since the Curie temperature increases with increasing metalloid content. Then with further increases in the annealing time, the number and volume of the crystallites increase, the amount of the original amorphous phase becomes smaller, and the new amorphous component develops that gradually becomes more uniform in composition.

After some time, the growth of the crystalline Fe-Si alloy slows down, and corresponds roughly to the disappearance of the original paramagnetic doublet. The remaining amorphous phase, which is magnetically split, then seems to be fairly uniform in composition and quasistable. A similar quasistable amorphous state was observed at room temperature in the earlier isochronal annealing experiments.[1] Once the amorphous phase becomes quasistable, further crystallization becomes more difficult.

During the slowing-down period, atomic rearrangements within the quasistable amorphous phase may be required before the onset of the second crystallization stage. Then, during this second stage, crystallization of Fe_2B commences and further crystallization of the Fe-Si alloy continues. The process by which Fe_3C crystallizes is unclear because the amount of this component present is so small.

ACKNOWLEDGMENT

This research was supported by a grant from the Natural Sciences and Engineering Research Council of Canada.

*Present address: Applied Physics Laboratory, Research Development Corporation of Japan, Hasunuma 1383-6, Oohomachi, Tsukuba, 300-32, Japan.

[1]N. Saegusa and A. H. Morrish, Phys. Rev. B 26, 305 (1982).

[2]D. C. Price, Aust. J. Phys. 34, 51 (1981).

[3]G. LeCaer, J. M. Dubois, and J. P. Senateur, J. Solid State Chem. 19, 19 (1976).

[4]M. Ron and Z. Mathalone, Phys. Rev. B 4, 774 (1971).

[5]W. Christian, *The Theory of Transformations in Metals and Alloys,* 2nd ed. (Pergamon, Oxford, 1975), Part I.

[6]A. S. Schaafsma, H. Snijders, and F. van der Woude, Phys. Rev. B 20, 4423 (1979).

[7]See, for example, V. R. V. Ramanan and G. E. Fish, J. Appl. Phys. 53, 2273 (1982).

[8]M. Mitera, T. Masumoto, and N. S. Kazama, J. Appl. Phys. 50, 7609 (1979); F. E. Luborsky and J. L. Walter, IEEE Trans. Magn. 16, 572 (1980).

[9]C. C. Tsuei and H. Lilienthal, Phys. Rev. B 13, 4899 (1978); J. Durand and M. F. Lapierre, J. Phys. F 6, 1185 (1976).

[10]N. Saegusa and A. H. Morrish, Phys. Rev. B 26, 10 (1982).

[11]J. C. Swartz, R. Kossowsky, J. J. Haugh, and R. F. Krause, J. Appl. Phys. 52, 3324 (1981); N. Saegusa and A. H. Morrish, J. Magn. Magn. Mater. (in press).